Vortex core states in superconducting graphene

I. M. Khaymovich,[1] N. B. Kopnin,[2,3] A. S. Mel'nikov,[1] and I. A. Shereshevskii[1]
[1]*Institute for Physics of Microstructures, Russian Academy of Sciences, GSP-105, 603950 Nizhny Novgorod, Russia*
[2]*Low Temperature Laboratory, Helsinki University of Technology, P.O. Box 2200, FIN-02015 HUT, Finland*
[3]*L. D. Landau Institute for Theoretical Physics, 117940 Moscow, Russia*
(Received 26 March 2009; published 8 June 2009)

The electronic structure of vortex states in superconducting graphene is studied within the Bogoliubov–de Gennes theory applied to excitations near the Dirac point. We consider the subgap spectrum transformations which occur with a change in the doping level. For an arbitrary vorticity and doping level we investigate the problem of existence of zero-energy modes. The crossover to a Caroli–de Gennes–Matricon type of spectrum is studied. Results of numerical computations are reported that illustrate the behavior of the spectrum with a change in the doping level.

DOI: 10.1103/PhysRevB.79.224506 PACS number(s): 73.63.−b, 74.25.Jb, 74.78.Na

I. INTRODUCTION

Recent exciting developments in transport experiments on graphene[1] have stimulated theoretical studies of possible superconductivity phenomena in this material.[2–5] Experimentally, there are both hints toward intrinsic superconductivity[6] and observations of proximity-induced superconductivity in graphene layers.[7] A number of unusual features of superconducting state have been predicted, which are closely related to the Dirac-like spectrum of normal-state excitations. In particular, the unconventional normal electron dispersion has been shown to result in a nontrivial modification of Andreev reflection[8] and Andreev bound states in Josephson junctions.[9] In this paper we consider another generic problem illustrating the new physics of Andreev scattering processes in graphene, namely, the electronic spectrum in the core of a vortex that can presumably appear in graphene-driven superconducting either via intrinsic or induced mechanism in the presence of magnetic field. The electronic vortex structure for Dirac fermions has been previously studied in particle physics for a situation equivalent to the zero doping limit in graphene, when the Dirac point lies exactly at the Fermi level. A number of important results have been obtained, namely, the exact solutions for the zero-energy modes[10,11] and the subgap spectrum for constant and linearly increasing gap profiles within the vortex core.[12] The problem of zero-energy modes has been further addressed in Ref. 13 for n-fold vortices in bilayer-graphene exciton condensate and in Ref. 14 for singly quantized vortices in various condensate phases described by the Dirac theory on a honeycomb lattice.

The energy spectrum is determined by the vortex winding number (vorticity) n and labeled by the angular-momentum ν which is a conserved quantity for an axisymmetric vortex. For zero doping the subgap spectrum consists of n zero-energy states.[10,11] The states with higher energies lie close to the gap edge $\pm|\Delta_0|$. Our goal here is to develop a theoretical description of the electronic structure of multiquantum vortices beyond the zero doping limit and study the transformation of the spectrum under the shift μ in the Fermi level from the Dirac point. We demonstrate that with an increase in doping level μ the distance between the energy levels decreases so that more and more states fill the subgap region. The set of low-energy levels gradually transforms into a set of n "spectrum branches" $E_n^{(i)}(\nu)$ where i assumes n integer values. If ν is considered as a continuous parameter, these n-energy branches cross the Fermi level[15] as functions of ν. The detailed behavior of the energy spectrum as a function of μ crucially depends on the parity of the winding number. For *odd* n there exists one branch, $E_n^{(0)}$, which intersects zero energy at $\nu=0$. Its crossing point belongs to the spectrum, thus resulting in an exact zero-energy mode. The crossing points of other $n-1$ branches do not generally belong to the spectrum for finite μ; thus, these zero modes do not exist. However, some of these $n-1$ zero-energy modes can appear again for certain doping levels. For high-doping $|\mu|\gg|\Delta_0|$, they appear almost periodically with an increase in the Fermi-momentum $\hbar k_F=|\mu|/v_F$ by a characteristic value $\delta k_F \sim 1/\xi$. Here ξ is a superconducting coherence length $\xi=\hbar v_F/\Delta_0$, and Δ_0 is a homogeneous gap value far from the vortex center. In a singly quantized vortex the energy spectrum for high doping is given by the Caroli–de Gennes–Matricon (CdGM) expression similar to that for usual s-wave superconductors.[16] For an *even* winding number the crossing points of all n branches do not generally belong to the spectrum if $\mu\neq 0$. In this case the exact zero modes are absent. Nevertheless, some of these zero-energy modes can appear again for certain μ in the way similar to the odd vorticity case. For high doping, they appear periodically with increasing μ. Indeed, the energy branches cross the Fermi level at certain momenta $\nu^{(i)}\sim k_F\xi$. The zero modes appear when these $\nu^{(i)}$ become integer (odd n) or half integer (even n) for discrete equally spaced (due to equidistant energy levels) values of the Fermi momentum. Because of the symmetry with respect to the sign of energy (see below) the zero-energy modes appear and disappear in pairs, for ν and $-\nu$.

The paper is organized as follows. In Sec. II we briefly discuss the basic equations used in our calculations. In Sec. III we analyze the general properties of the zero-energy modes and find the exact solution for the $\nu=0$ zero-energy level in an odd-quantum vortex. In Sec. IV we consider the large doping limit and derive the quasiclassical equations describing the quantum mechanics of quasiparticles in superconducting graphene. We also use these equations to study the vortex core states in the large μ limit. In Sec. V we

present our numerical results and compare them with the analytical findings. We summarize our results in Sec. VI.

II. BASIC EQUATIONS

The Bogoliubov–de Gennes (BdG) equations in superconducting graphene for energies close to the Dirac points can be written as two decoupled sets of four equations each.[8] Assuming valley degeneracy, it is sufficient to consider only one of these sets,

$$v_F\hat{\boldsymbol{\sigma}}\cdot\left(\check{\mathbf{p}}-\frac{e}{c}\mathbf{A}\right)\hat{u}+\Delta\hat{v}=(E+\mu)\hat{u}, \tag{1}$$

$$-v_F\hat{\boldsymbol{\sigma}}\cdot\left(\check{\mathbf{p}}+\frac{e}{c}\mathbf{A}\right)\hat{v}+\Delta^*\hat{u}=(E-\mu)\hat{v}, \tag{2}$$

known as "Dirac-BdG equations."[8,17] Here $\check{\mathbf{p}}=-i\hbar\boldsymbol{\nabla}$ while $\hat{u}=(u_1,u_2)$ and $\hat{v}=(v_1,v_2)$ are two-component wave functions of electrons and holes in different valleys in the Brillouin zone[18] (indices 1 and 2 denote two sublattices of the honeycomb structure). They form spinors in the pseudospin space in which the Pauli matrices $\hat{\sigma}_x$, $\hat{\sigma}_y$, and $\hat{\sigma}_z$ are defined; we also introduce a vector $\hat{\boldsymbol{\sigma}}=(\hat{\sigma}_x,\hat{\sigma}_y)$. The energy is measured from the Fermi level. For zero doping, $\mu=0$, the Fermi level lies exactly at the Dirac point. For a finite doping, the Fermi level is shifted by $\mu>0$ upwards (electron doping) or downwards $\mu<0$ (hole doping) from the Dirac point. The doping level μ is assumed to be much smaller than the bandwidth D of the normal-state electronic spectrum such that the coupling between the valleys can be ignored. Equations (1) and (2) also disregard the effects of the true electronic spin together with the Zeeman splitting of levels. For a homogeneous gap $\Delta=\Delta_0$ and zero magnetic field the wave functions take the form of plane waves $\hat{u},\hat{v}\propto e^{i\mathbf{p}\cdot\mathbf{r}}$, and we obtain two noninteracting energy branches $E^2=\Delta_0^2+(\mu\mp v_Fp)^2$, which correspond to the pseudospin orientation parallel and antiparallel to the momentum direction, respectively.

For an axisymmetric n-quantum vortex one can choose the gauge $A_\rho=0$ and $A_\phi=A_\phi(\rho)$ and put $\Delta=|\Delta(\rho)|e^{in\phi}$, where ρ,ϕ are cylindrical coordinates and the function $A_\phi(\rho)$ is determined by the magnetic field profile. The resulting eigenstates are labeled by a discrete angular-momentum quantum number ν,

$$\begin{pmatrix}\hat{u}\\ \hat{v}\end{pmatrix}=e^{i\nu\phi-i\hat{\sigma}_z\phi/2+i\hat{\sigma}_z\pi/4}\begin{pmatrix}e^{in\phi/2}\hat{U}(\rho)\\ e^{-in\phi/2}\hat{V}(\rho)\end{pmatrix}. \tag{3}$$

The extra factor $e^{-i\hat{\sigma}_z\phi/2}$ as compared to the usual BdG functions u and v comes from the angular dependence of the momentum operator in cylindrical coordinates,

$$\check{p}_x\pm i\check{p}_y=e^{\pm i\phi}\hbar[-i\,\partial/\partial\rho\pm\rho^{-1}\,\partial/\partial\phi].$$

After rotation of the coordinate system around the vortex axis by the angle $\delta\phi=2\pi$ the wave functions acquire the phase-factor $e^{2\pi i\nu+i\pi(n-1)}$, as distinct from the standard CdGM-factor $e^{2\pi i\nu+i\pi n}$. Thus, the transformation properties of the wave functions under rotation around the vortex axis correspond to those for an s-wave superconductor with the replacement $n\to n-1$. The wave function should be single valued, and this condition gives us a restriction on possible ν values. One can see that ν should be half integer for even vorticity n and integer for odd n in contrast to standard s-wave superconductors.

III. GENERAL PROPERTIES OF ZERO ENERGY STATES

Equations (1) and (2) are invariant under the transformation

$$E\to -E,\quad i\hat{\sigma}_y\hat{u}^*\to\hat{v},\quad i\hat{\sigma}_y\hat{v}^*\to-\hat{u}. \tag{4}$$

Thus, for arbitrary vorticity and doping level, a set of zero-energy modes $(\hat{u}_i,\hat{v}_i)$ labeled by an index i satisfies[10] $\hat{v}_i=i\hat{\sigma}_y\hat{u}_j^*$, $\hat{u}_i=-i\hat{\sigma}_y\hat{v}_j^*$. This transformation couples the states with opposite angular momenta. One can separate two types of zero-energy solutions: (i) the eigenfunction components transform into each other, $i=j$, which can be realized only for $\nu=0$. (ii) There exists a pair of eigenfunctions $i\neq j$ with opposite $\nu\neq0$ coupled by the above transformation.

Consider solutions of the first type which can exist only for an odd-quantum vortex. We put $\hat{v}=i\hat{\sigma}_y\hat{u}^*$ and find

$$\left[v_F\hat{\boldsymbol{\sigma}}\cdot\left(\check{\mathbf{p}}-\frac{e}{c}\mathbf{A}\right)-\mu\right]\hat{u}+i\Delta\hat{\sigma}_y\hat{u}^*=0. \tag{5}$$

We look for the solution in the form $\hat{u}=\zeta(\rho)\hat{U}^{(0)}$, where $\hat{U}^{(0)}$ satisfies Eq. (5) with $\Delta=0$; ζ is a real function satisfying

$$\hat{\sigma}_xe^{i\hat{\sigma}_z\phi}\hat{U}^{(0)}\hbar v_F(d\zeta/d\rho)=\hat{\sigma}_y\hat{U}^{(0)*}\Delta\zeta.$$

One can assume that the magnetic field in a thin graphene layer is nearly homogeneous. As in the standard problem of an electron in a homogeneous magnetic field, the normal-state function $\hat{U}^{(0)}$ diverges at large distances ρ on the order of the magnetic length $L_H=\sqrt{\hbar c/|eH|}$ due to the growing vector potential $A_\phi=H\rho/2$ except for a discrete set of $\mu=\pm\sqrt{2|eH|\hbar v_F^2k/c}$ which correspond to the Landau energy levels (see the Appendix). However, similar to the case of the usual superconductors, the superconducting velocity proportional to $\mathbf{A}-(\hbar c/2e)\boldsymbol{\nabla}\chi$, with χ being the order-parameter phase, is finite in the vortex state due to the presence of the vortex lattice. Therefore, this large-distance divergence is cut off either at the intervortex distance $\sim L_H$ (flux lattice) or at the magnetic field screening length (isolated vortex). Since the magnetic field near the vortex core is rather weak $H\ll H_{c2}$ the magnetic length greatly exceeds the coherence length, $L_H\gg\xi=\hbar v_F/\Delta_0$. Therefore, for the states localized near the vortex core at distances on the order of ξ we can disregard the above-mentioned divergence and even neglect the vector potential at all. In this way we obtain for $\mu>0$,

$$\hat{U}^{(0)}=C\begin{pmatrix}e^{-i\pi/4}e^{i(n-1)\phi/2}J_{(n-1)/2}(k_F\rho)\\ e^{+i\pi/4}e^{i(n+1)\phi/2}J_{(n+1)/2}(k_F\rho)\end{pmatrix},$$

where C is a real constant, $k_F=\mu/\hbar v_F$, and

$$\zeta(\rho)=e^{-K(\rho)};\quad K(\rho)=\frac{1}{\hbar v_F}\int_0^\rho|\Delta(\rho')|d\rho'. \tag{6}$$

For $n=1$ this coincides with the result of Ref. 14.

To address the problem of the zero-energy solutions of the second type for $\nu \neq 0$ we note that the symmetry transformation [Eq. (4)] implies that under the transformation $E \to -E$ and $\nu \to -\nu$ the functions $\hat{U}$ and $\hat{V}$ in Eq. (3) change according to $V_2 \to U_1$ and $V_1 \to -U_2$. Therefore, for $E=0$, the functions with opposite momenta coupled by Eq. (4) obey $V_{2,\nu} = U_{1,-\nu}$, and $V_{1,\nu} = -U_{2,-\nu}$. Equations for U_1 and U_2 take the form

$$\left(\frac{d}{d\rho} - \frac{N_-}{\rho} + \frac{eA_\phi}{\hbar c}\right)U_{1,\nu} + \frac{|\Delta|}{\hbar v_F}U_{1,-\nu} = \frac{\mu}{\hbar v_F}U_{2,\nu}, \tag{7}$$

$$\left(\frac{d}{d\rho} + \frac{N_+}{\rho} - \frac{eA_\phi}{\hbar c}\right)U_{2,\nu} + \frac{|\Delta|}{\hbar v_F}U_{2,-\nu} = -\frac{\mu}{\hbar v_F}U_{1,\nu}. \tag{8}$$

Here $N_\pm = \nu + (n \pm 1)/2$ and $A_\phi(\rho)$ is the ϕ component of the vector potential. We multiply the first equation with $U_{2,\nu}$ and the second one with $U_{1,\nu}$. Next we do the same for the opposite sign of ν and then add all the resulting equations together. We thus find

$$\mu \int_0^\infty (U_{2,\nu}^2 - U_{2,-\nu}^2 - U_{1,\nu}^2 + U_{1,-\nu}^2)\rho d\rho = \hbar v_F \int_0^\infty \frac{d}{d\rho}[\rho(U_{1,\nu}U_{2,\nu} - U_{1,-\nu}U_{2,-\nu})]d\rho. \tag{9}$$

For a solution regular at the origin and decaying at $\rho \to \infty$ the right-hand side (rhs) of Eq. (9) is zero and thus, the left-hand side (lhs) of this equation also should vanish. One can see that for $\nu \neq 0$ and $\mu \neq 0$, the lhs is nonzero in general. Therefore, zero-energy levels do not generally exist.

To illustrate this we analyze the case of small μ using the perturbation theory. For $\mu=0$ the equation for U_1 decouples from that of U_2. As follows from Ref. 10 for positive circulation $n \geq 1$, the functions $U_{1,\nu}$ are regular while $U_{2,\nu}=0$ if $-\frac{1}{2}(n-1) \leq \nu \leq \frac{1}{2}(n-1)$. For negative circulation, the functions $U_{2,\nu}$ are regular while $U_{1,\nu}=0$ if $\frac{1}{2}(n+1) \leq \nu \leq -\frac{1}{2}(n+1)$. In total there exist $|n|$ zero-energy levels. For small μ we can calculate the integral in the lhs of Eq. (9) using the wave functions satisfying Eqs. (7) and (8) with $\mu=0$. Using the results of Ref. 10 for $n>0$, one can check that $U_\nu^2 - U_{-\nu}^2$ is nonzero unless $\nu=0$. Therefore, there is no decaying solution and, thus, there is no zero-energy level for small μ and $\nu \neq 0$. However, the zero-energy levels may appear occasionally for certain finite values of μ, as it is shown below.

IV. QUASICLASSICAL APPROACH FOR LARGE DOPING LEVELS

The limit of large μ is very instructive and helps to get the complete picture of the spectrum transformation. For the analysis we follow a standard quasiclassical scheme (see Ref. 20 for details) and introduce a momentum representation

$$\psi(\rho) = (2\pi\hbar)^{-2}\int d^2 p e^{i\mathbf{p}\boldsymbol{\rho}/\hbar}\psi(\mathbf{p}),$$

where $\mathbf{p} = p(\cos\theta_p, \sin\theta_p)$. Let us transform the wave functions so to choose the pseudospin quantization axis along the direction of the momentum $\mathbf{p}$: $\hat{u} = \hat{S}\hat{g}_u$, $\hat{v} = \hat{S}\hat{g}_v$, where

$$\hat{S} = e^{-i\theta_p\hat{\sigma}_z/2}(\hat{\sigma}_z + \hat{\sigma}_x)/\sqrt{2},$$

$$\hat{S}^+ = (\hat{\sigma}_z + \hat{\sigma}_x)e^{i\theta_p\hat{\sigma}_z/2}/\sqrt{2}.$$

Equations (1) and (2) take the form

$$[v_F\hat{\sigma}_z p - \mu]\hat{g}_u + \hat{h}_{\check{A}}\hat{g}_u + \hat{h}_{\check{\Delta}}\hat{g}_v = E\hat{g}_u, \tag{10}$$

$$[\mu - v_F\hat{\sigma}_z p]\hat{g}_v + \hat{h}_{\check{A}}\hat{g}_v + \hat{h}_{\check{\Delta}}^+\hat{g}_u = E\hat{g}_v, \tag{11}$$

where we define the operators

$$\hat{h}_{\check{\Delta}} = \hat{S}^+\check{\Delta}\hat{S}, \quad \hat{h}_{\check{\Delta}}^+ = \hat{S}^+\check{\Delta}^+\hat{S},$$

$$\hat{h}_{\check{A}} = -(ev_F/c)\hat{S}^+\hat{\boldsymbol{\sigma}}\check{\mathbf{A}}\hat{S}.$$

Here $\check{\mathbf{A}} = \mathbf{A}(\check{\boldsymbol{\rho}})$ and $\check{\Delta} = \Delta(\check{\boldsymbol{\rho}})$ are functions of the coordinate operator $\check{\boldsymbol{\rho}} = i\hbar\partial/\partial\mathbf{p}$. Generally, the operators $\hat{h}_{\check{A}}$ and $\hat{h}_{\check{\Delta}}$ mix the energy bands with opposite pseudospin orientations. However, in the limit of large positive chemical-potential $\mu \gg \Delta_0$ for the subgap spectrum one can adopt the single-band approximation with a fixed pseudospin orientation

$$\hat{\sigma}_z\hat{g}_u = \hat{g}_u = g_u(1,0),$$

$$\hat{\sigma}_z\hat{g}_v = \hat{g}_v = g_v(1,0).$$

The accuracy of such approximation can be determined using the second-order perturbation theory; the corresponding corrections to the energy caused by the off-diagonal pseudospin terms in $\hat{h}_{\check{A}}$ and $\hat{h}_{\check{\Delta}}$ are

$$\delta E_A \sim (\xi^4/L_H^4)(\Delta_0/k_F\xi),$$

$$\delta E_\Delta \sim \Delta_0/(k_F\xi)^3.$$

These corrections are much smaller that the proper energy scale $\Delta_0/k_F\xi \sim \Delta_0^2/\mu$ for the subgap spectrum. One concludes therefore that the single-band approximation is sufficient for the case of large doping $\mu \gg \Delta$. The assumption of large $\mu > 0$ allows us to consider only the momenta close to $\hbar k_F$. Thus, we put $p = \hbar k_F + q$ ($|q| \ll \hbar k_F$) and perform a Fourier transformation into the (s, θ_p) representation

$$\bar{g}(\mathbf{p}) = \begin{pmatrix} g_u \\ g_v \end{pmatrix} = k_F^{-1}\int_{-\infty}^{+\infty} ds e^{-iqs/\hbar}\bar{g}(s,\theta_p). \tag{12}$$

We introduce here the vector $\bar{g}$ and Pauli matrices $\bar{\tau}_x, \bar{\tau}_y, \bar{\tau}_z$ in electron-hole space.

A. Type I levels in an odd-quantum vortex

We start with an odd-quantum vortex and consider the low-energy levels of the first kind which belong to the anomalous energy-branch $E_n^{(0)}$ crossing the Fermi level at $\nu = 0$. To find the solution for angular-momenta $\nu/k_F\xi \ll 1$ we take the coordinate operator in the s, θ_p representation

$$\hat{\mathbf{r}} = s\mathbf{k}_F/k_F + \{[\mathbf{k}_F \times \mathbf{z}_0], \hat{\nu}\}/(2k_F^2)$$

where $\{A,B\}=AB+BA$ is an anticommutator. For small $\nu/k_F\xi \ll 1$ we can use a linear expansion of $\hat{h}_{\check{A}}$ and $\hat{h}_{\check{\Delta}}$ in terms of the angular-momentum operator $\check{\nu}=-i\partial/\partial\theta_p$

$$\hat{h}_A = -\frac{eHv_F}{4ck_F} e^{-i\theta_p/2}\{\hat{\nu}, e^{i\theta_p}\}e^{-i\theta_p/2},$$

$$\hat{h}_\Delta = \frac{\Delta_0 f(|s|)}{|s|}\left[se^{i\eta\theta_p} - \frac{i}{4k_F}\sum_{k=0}^{n-1} e^{i(k-1/2)\theta_p} \times \{e^{i\theta_p}, \{\hat{\nu}, e^{i\theta_p}\}\} e^{i(n-k-3/2)\theta_p}\right].$$

Taking $\bar{g}(s,\theta_p)=\exp(i\nu\theta_p+i\bar{\tau}_z n\theta_p/2)\bar{F}(s)$ and assuming a small homogeneous magnetic field, we obtain

$$-i\hbar v_F\bar{\tau}_z\frac{\partial\bar{F}}{\partial s} + |\Delta(s)|\left[\frac{s}{|s|}\bar{\tau}_x + \frac{\nu n}{|s|k_F}\bar{\tau}_y\right]\bar{F} = E'\bar{F}, \quad (13)$$

where $E'=E+\nu\hbar\omega_c/2$ and $\omega_c=eHv_F/c\hbar k_F$ is the cyclotron frequency. Considering the last term in the above Hamiltonian as a perturbation we find

$$E_n^{(0)} = -\nu\left[\frac{n}{Ik_F}\int_0^\infty \frac{|\Delta(s)|}{s} e^{-2K(s)}ds + \frac{\hbar\omega_c}{2}\right], \quad (14)$$

where $I=\int_0^\infty \zeta^2(s)ds$ while $K(s)$ and $\zeta(s)$ are defined by Eq. (6). Equation (14) corresponds to the CdGM result[16] with an account of a magnetic field in the spirit of Ref. 19. Note that ν is an integer for odd-quantum vortex. Since ν can now take zero value, the spectrum has a zero-energy mode.

B. Type II levels for $\nu \neq 0$

The levels of both first and second types for any vorticity n can be easily described in the limit of large $\nu \gg 1$. In Eqs. (10) and (11) we can then replace the angular-momentum operator by a classical continuous variable. Instead of Eq. (13) we get the Andreev equations along the rectilinear quasiclassical trajectories

$$\left[-i\hbar v_F\bar{\tau}_z\frac{\partial}{\partial s} + \frac{\hbar\omega_c k_F b}{2} + \bar{D}(\boldsymbol{\rho}) - E\right]\bar{g}(s,\theta_p) = 0, \quad (15)$$

where $\bar{D}=\bar{\tau}_x \mathrm{Re}\,\Delta(\boldsymbol{\rho})-\bar{\tau}_y \mathrm{Im}\,\Delta(\boldsymbol{\rho})$, $b=-\nu/k_F$ is the trajectory impact parameter, and the position vector on the trajectory is

$$\boldsymbol{\rho} = (s\cos\theta_p - b\sin\theta_p, s\sin\theta_p + b\cos\theta_p).$$

Equation (15) describes the quasiparticle states in an arbitrary gap profile. For the particular case of a multiquantum vortex the gap operator in Eq. (15) takes the form

$$\Delta(\boldsymbol{\rho}) = |\Delta(\sqrt{s^2+b^2})|\left[\frac{s+ib}{\sqrt{s^2+b^2}}\right]^n e^{in\theta_p}.$$

The total wave function should be single valued. The appropriate Bohr-Sommerfeld quantization rule reads

$$k_F\int_0^{2\pi} b(\theta_p)d\theta_p = 2\pi m + \pi(n-1),$$

where m is an integer. The last term accounts for all the phase factors that appear in $\hat{S}$ and $\hat{g}$. As a result, the angular-momentum ν should be integer or half integer for odd and even vorticity, respectively. This agrees with the conditions imposed by Eq. (3).

For $|E|<\Delta_0$ the solution of corresponding Andreev equations is known to give $|n|$ anomalous energy-branches $E_n^{(i)}(b)$ crossing zero energy as functions of continuous parameter b (see Refs. 15 and 20 and references therein). The analytical expressions describing these branches in the region $E \ll \Delta_0$ are determined by[20]

$$E_n^{(\alpha)} = \frac{\int_0^\infty \left[G_I^{(\alpha)}(s) - 2\alpha G_R^{(\alpha)}(s)\arctan\frac{s}{b}\right]e^{-2K_\alpha(s)}ds}{\int_0^\infty e^{-2K_\alpha(s)}ds} + \frac{\hbar\omega_c k_F b}{2}, \quad (16)$$

where

$$K_\alpha(s) = \frac{1}{\hbar v_F}\int_0^s G_R^{(\alpha)}(t)dt, \quad (17)$$

$$G_R^{(\alpha)} = |\Delta(\sqrt{s^2+b^2})|\mathrm{Re}\left\{\left[\frac{s+ib}{\sqrt{s^2+b^2}}\right]^{n-2\alpha}\right\}, \quad (18)$$

$$G_I^{(\alpha)} = |\Delta(\sqrt{s^2+b^2})|\mathrm{Im}\left\{\left[\frac{s+ib}{\sqrt{s^2+b^2}}\right]^{n-2\alpha}\right\}. \quad (19)$$

For $n>0$ ($n<0$) the values of α are such that $\alpha \geq 0$ ($\alpha \leq 0$) and $n-2\alpha$ is an odd positive (negative) integer. The term with $\arctan(s/b)$ in Eq. (16) has a discontinuity at $b=0$. Therefore, there are two different branches of the energy spectrum for each $\alpha \neq 0$, which yields total $|n|$ energy branches crossing zero as functions of b.

Especially simple expression is obtained for a singly quantized vortex ($n=1$) if we assume the order parameter in the form $\Delta(r)=\Delta_0 r/\sqrt{r^2+\xi^2}$. With $\alpha=0$ we get an explicit expression for the CdGM spectrum,

$$E_1^{(0)} = \frac{\Delta_0 b}{\sqrt{b^2+\xi^2}}\frac{\mathcal{K}_0(2\sqrt{(b/\xi)^2+1})}{\mathcal{K}_1(2\sqrt{(b/\xi)^2+1})}, \quad (20)$$

where $\mathcal{K}_m$ is the McDonald function.

Equation (16) for the anomalous branches at low energies take the form $E^{(\alpha)}(b)\sim\Delta_0(b-b_\alpha)/\xi$, where $-\xi \lesssim b_\alpha \lesssim \xi$. For the branches with $b_i \neq 0$ the change in the Fermi momentum is accompanied by the flow of the eigenvalues through the Fermi level: the energy levels cross it by pairs at discrete values $k_F=|\nu/b_\alpha|$. For $\nu\to 0$, expression (16) describing the branch crossing the Fermi level at zero impact parameter (levels of the first kind) transforms into Eq. (14). In general, Eq. (16) provides a good approximation for the spectrum for

all branches and impact parameters as can be seen from the numerical results discussed in the next section.

V. NUMERICAL RESULTS

The above analytical considerations are in excellent agreement with our numerical calculations. We choose the vortex position at the disk center and approximate the gap function of n-quantum vortex by the expression

$$\Delta(\rho) = \Delta_0 e^{in\phi}\left[\frac{\rho}{\sqrt{\rho^2+\xi^2}}\right]^n.$$

In principle, the gap-profile $|\Delta(\rho)|$ has to be calculated self-consistently. These calculations will be done elsewhere. The self-consistency procedure will result, of course, in some modifications of the gap profile. For example, vortex core shrinking and Friedel-type oscillations in the pair potential may appear in a way similar to the results known for standard superconductors (see, e.g., Ref. 21). However, the shape of the gap profile is known to affect only slightly the quasiparticle energies; it does not change the key features of the vortex core states which are controlled by the vortex topology.[15] Therefore, the adopted approximation is expected to closely reproduce the true core spectrum and the wave functions.

For numerical solution, Eqs. (1) and (2) are expanded in the basis of eigenfunctions of a normal graphene disk of radius R. We are not interested here in the effect of boundaries on the subgap spectrum and thus, for the sake of simplicity we use the conditions of zero current through the disk boundary in the following form:

$$u_1(R) = 0, \quad v_1(R) = 0. \tag{21}$$

To suppress the influence of the boundary conditions the radius R is taken much larger than the eigenfunction decay length in the superconducting phase, i.e., the coherence-length ξ. Note that for the sake of simplicity we also neglected the small corrections to the spectrum associated with the finite magnetic field. The electronic and hole normal-state eigenfunctions satisfying the above boundary conditions take the form

$$\hat{U}^e_{\nu,p} \propto \hat{U}^{(0)}_{m_e,p}(\rho), \quad \hat{V}^e_{\nu,p} = 0, \tag{22}$$

$$\hat{U}^h_{\nu,p} = 0, \quad \hat{V}^h_{\nu,p} \propto \hat{U}^{(0)}_{m_h,p}(\rho), \tag{23}$$

where

$$\hat{U}^{(0)}_{m,p}(\rho) = \begin{pmatrix} J_m(k^m_p\rho) \\ -J_{m+1}(k^m_p\rho) \end{pmatrix},$$

m is either m_e or m_h, $m_{e,h}=\nu-(1\mp n)/2$, and $k^m_p R$ are the p-th zeros of the Bessel function $J_m(x)$. In a finite-size disk the basis also includes electronic and hole functions (22) and (23) with

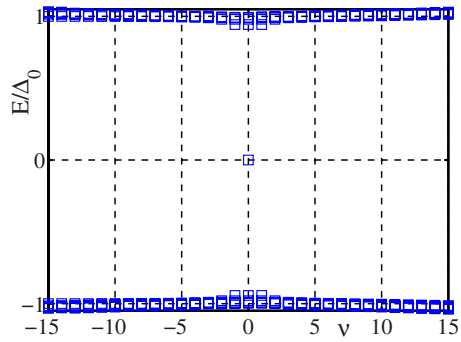

FIG. 1. (Color online) The subgap spectrum vs the angular momentum ν for a singly quantized vortex at zero-doping level. We choose here $R/\xi=100$.

$$\hat{U}^{(0)}_{m,0}(\rho) = \begin{pmatrix} 0 \\ \rho^{-m-1} \end{pmatrix},$$

which is finite at the origin for $m_{e,h}\leq -1$, respectively, and correspond to $k^{m_{e,h}}_0=0$. For numerical diagonalization the matrix is truncated keeping the number of eigenstates larger than $10R/\xi$.

The calculations carried out for zero-doping level $\mu=0$ give us the zero-energy mode in a singly quantized vortex (see Fig. 1). All other subgap levels in this case appear to be very close to the gap value in a qualitative agreement with the model calculations[12] based on the assumption of the constant profile of the gap-function $|\Delta(\rho)|=\Delta_0$. Shown in Fig. 2 are typical energy spectra for singly and doubly quantized

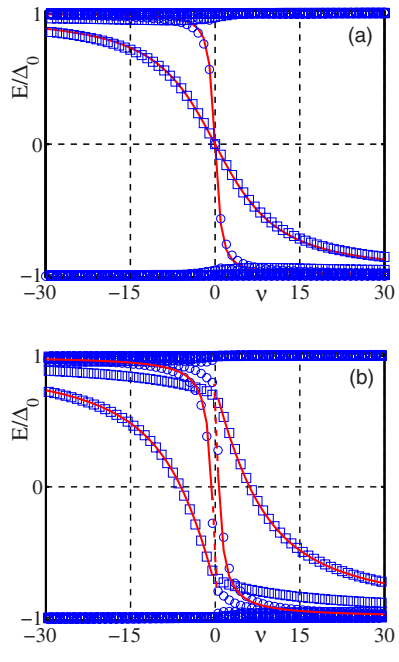

FIG. 2. (Color online) The subgap spectrum vs the angular-momentum ν for singly (a) and doubly (b) quantized vortices in superconducting graphene with different doping levels: $\mu/\Delta_0=1$ (circles) and $\mu/\Delta_0=10$ (squares). The quasiclassical solutions [Eq. (16)] for $\omega_c\to 0$ are shown by solid lines (dashed parts of lines are guides for the eyes). We choose here $R/\xi=100$.

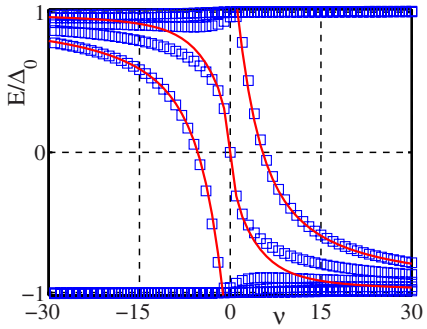

FIG. 3. (Color online) The subgap spectrum vs the angular momentum ν for a vortex with $n=3$. The quasiclassical analytical solutions [Eq. (16)] for $\omega_c \to 0$ are shown by solid lines. We choose here $R/\xi=100$ and $\mu/\Delta_0=5$.

vortices calculated for different doping levels. In Fig. 3 we present the spectral branches for a vortex with the winding number $n=3$. Spectrum consists of anomalous branches crossing zero of energy and branches lying close to the gap edges. Figures 2 and 3 clearly demonstrate the difference between odd and even vorticities. Figure 2(a) illustrates also a crossover to a spectrum of the CdGM type with increasing doping level. For large μ all anomalous branches for different vorticities are well described by the quasiclassical Eq. (16) obtained in Ref. 20.

VI. CONCLUSIONS

In an *s*-wave superconducting graphene the subgap spectrum in a vortex core has a set of energy branches that cross Fermi level as functions of ν treated as a continuous parameter. The number of the branches is determined by the vortex winding number n. Whether the crossing points of these branches with zero belong to the energy states or not depends on the parity of the vortex and on the doping level μ. For a degenerate case $\mu=0$ there are $|n|$ zero-energy levels, i.e., all crossing points belong to the spectrum. If the doping level μ is increased, the spectrum transformation depends strongly on the parity of the vortex. (i) For an odd winding number one of the zero-energy modes (type I mode), i.e., that with $\nu=0$, survives with an increase in μ. The other $|n|-1$ (i.e., even number of) levels split-off zero with increasing μ (type II modes). (ii) For even-quantum vortex, all $|n|$ levels belong to the second type and splitoff zero. In general, the zero-energy modes of the second type can appear or disappear with the change in μ and may exist only in pairs. Finally, we recall that μ is much smaller than the bandwidth D. The valley symmetry implied in Eqs. (1) and (2) results, of course, in a twofold degeneracy of the energy levels. If μ is increased up to much higher values $\sim D$ this degeneracy is lifted and the zero modes can be split.[14] Also, Eqs. (1) and (2) ignore the effects of true electronic spin which would result in a standard Zeeman splitting of all energy levels.[11,14,19]

ACKNOWLEDGMENTS

We are thankful to G. E. Volovik for many stimulating discussions. This work was supported in part by the Russian Foundation for Basic Research, the "Dynasty" Foundation, and the Academy of Finland (ASM).

APPENDIX: NORMAL STATE IN A HOMOGENEOUS MAGNETIC FIELD

Let us consider a homogeneous magnetic field along the z axis: $\mathbf{H}=\mathbf{z}_0 H$. We choose the gauge $A_\phi=H\rho/2$. Equation (5) in the normal-state,

$$\left[v_F \hat{\boldsymbol{\sigma}} \cdot \left(\check{\mathbf{p}} - \frac{e}{c}\mathbf{A} \right) - \mu \right] \hat{U}^{(0)} = 0,$$

has a general solution

$$\hat{U}^{(0)} = C e^{i/2n\phi - i/2\hat{\sigma}_z(\phi+\pi/2)} t^{|n-\hat{\sigma}_z|/2} e^{-t^2/4} \cdot \hat{f}(t), \qquad \text{(A1)}$$

Here $t=\rho/L_H$, $L_H=\sqrt{\hbar c/|eH|}$ is the magnetic length, n is an odd integer, and

$$\hat{f}(t) = \begin{pmatrix} A_1 M(a_1,b_1,t^2/2) \\ A_2 M(a_2,b_2,t^2/2) \end{pmatrix}.$$

We put

$$a_{1,2} = \frac{1}{4}[|n \mp 1| + 2 - (n \pm 1)\mathrm{sign}(eH) - 2\tilde{\mu}^2],$$

$$b_{1,2} = \frac{1}{2}[|n \mp 1|] + 1,$$

$\tilde{\mu}=\mu L_H/\hbar v_F$, and

$$A_2 = -A_1 \ \mathrm{sign}(n)[\sqrt{2}\tilde{\mu}/(|n|+1)]^{\mathrm{sign}(n)}.$$

$M(a,b,z)$ is the confluent hypergeometric function of the first kind, i.e., Kummer's function (see Ref. 22), and C is a constant.

The leading term in the asymptotic expansion of the function $\hat{f}$ at large distances is

$$\hat{f}(t \to \infty) = e^{t^2/2} \begin{pmatrix} A_1 \frac{\Gamma(b_1)}{\Gamma(a_1)} \left(\frac{t^2}{2}\right)^{a_1-b_1} \\ A_2 \frac{\Gamma(b_2)}{\Gamma(a_2)} \left(\frac{t^2}{2}\right)^{a_2-b_2} \end{pmatrix}, \qquad \text{(A2)}$$

where Γ is the Gamma function. For $a_{1,2}=-k_{1,2}$ (where $k_{1,2} \geq 0$ are integers) this term vanishes since the functions $\Gamma(a_{1,2})$ have poles. As a result, the solution $\hat{U}^{(0)}$ decays at $\rho \to \infty$. This condition yields the well-known Landau levels[23] for Dirac electrons with zero mass, i.e., for Eq. (5) with $\Delta=0$: $\tilde{\mu}=\pm\sqrt{2k}$, where $k=0,1,2\ldots$.

[1] K. S. Novoselov, A. K. Geim, S. V. Morozov, D. Jiang, M. I. Katsnelson, I. V. Grigorieva, S. V. Dubonos, and A. A. Firsov, Nature (London) **438**, 197 (2005).
[2] B. Uchoa and A. H. Castro Neto, Phys. Rev. Lett. **98**, 146801 (2007).
[3] A. M. Black-Schaffer and S. Doniach, Phys. Rev. B **75**, 134512 (2007).
[4] C. Honerkamp, Phys. Rev. Lett. **100**, 146404 (2008).
[5] N. B. Kopnin and E. B. Sonin, Phys. Rev. Lett. **100**, 246808 (2008).
[6] Y. Kopelevich and P. Esquinazi, J. Low Temp. Phys. **146**, 629 (2007); P. Esquinazi, N. Garcia, J. Barzola-Quiquia, P. Rodiger, K. Schindler, J.-L. Yao, and M. Ziese, Phys. Rev. B **78**, 134516 (2008).
[7] H. B. Heersche, P. Jarillo-Herrero, J. B. Oostinga, L. M. K. Vandersypen, and A. F. Morpurgo, Solid State Commun. **143**, 72 (2007); T. Sato, T. Moriki, S. Tanaka, A. Kanda, H. Miyazaki, S. Odaka, Y. Ootuka, K. Tsukagoshi, and Y. Aoyagi, Physica E (Amsterdam) **40**, 1495 (2008).
[8] C. W. J. Beenakker, Phys. Rev. Lett. **97**, 067007 (2006); Rev. Mod. Phys. **80**, 1337 (2008).
[9] M. Titov, A. Ossipov, and C. W. J. Beenakker, Phys. Rev. B **75**, 045417 (2007).
[10] R. Jackiw and P. Rossi, Nucl. Phys. B **190**, 681 (1981).
[11] P. Ghaemi and F. Wilczek, arXiv:0709.2626 (unpublished).
[12] B. Seradjeh, Nucl. Phys. B **805**, 182 (2008).
[13] B. Seradjeh, H. Weber, and M. Franz, Phys. Rev. Lett. **101**, 246404 (2008).
[14] D. Bergman and K. Le Hur, arXiv:0806.0379, Phys. Rev. B (to be published).
[15] G. E. Volovik, Pis'ma Zh. Eksp. Teor. Fiz. **57**, 233 (1993) [JETP Lett. **57**, 244 (1993)]; *The Universe in a Helium Droplet* (Oxford University Press, New York, 2003).
[16] C. Caroli, P. G. de Gennes, and J. Matricon, Phys. Lett. **9**, 307 (1964).
[17] B. Uchoa, G. G. Cabrera, and A. H. Castro Neto, Phys. Rev. B **71**, 184509 (2005).
[18] A. H. Castro Neto, F. Guinea, N. M. Peres, K. S. Novoselov, and A. K. Geim, Rev. Mod. Phys. **81**, 109 (2009).
[19] E. Brun Hansen, Phys. Lett. **27**, 576 (1968).
[20] A. S. Mel'nikov, D. A. Ryzhov, and M. A. Silaev, Phys. Rev. B **78**, 064513 (2008).
[21] L. Kramer and W. Pesch, Z. Phys. **269**, 59 (1974); N. Hayashi, T. Isoshima, M. Ichioka, and K. Machida, Phys. Rev. Lett. **80**, 2921 (1998).
[22] *Handbook of Mathematical Functions*, Natl. Bur. Stand. Appl. Math. Ser., Spec. Publ. No. 55, edited by M. Abramowitz and I. A. Stegun (U.S. GPO, Washington, DC, 1965).
[23] A. I. Akhiezer and V. B. Berestetsky, *Quantum Electrodynamics* (Interscience Publishers, New York, 1965).